HTML ABSTRACT + LINKS

Atomic layer deposition of hafnium oxide on germanium substrates

Annelies Delabie, Riikka L. Puurunen,[a] Bert Brijs, Matty Caymax,[b] Thierry Conard, Bart Onsia, Olivier Richard, Wilfried Vandervorst,[a] Chao Zhao, Marc M. Heyns, and Marc Meuris
Interuniversity Micro Electronics Center (IMEC), Kapeldreef 75, B-3001 Leuven, Belgium

Minna M. Viitanen, Hidde H. Brongersma, and Marco de Ridder
Calipso bv, Den Dolech 2, Postbus 513, 5600 MB Eindhoven, The Netherlands

Lyudmila V. Goncharova, Eric Garfunkel, and Torgny Gustafsson
Department of Physics and Astronomy and of Chemistry, and Laboratory for Surface Modification, Rutgers University, 136 Frelinghuysen Road, Piscataway, New Jersey 08854

Wilman Tsai
Intel Corporation, SC1-05, 2200 Mission College Boulevard, Santa Clara, California 95054-1549

(Received 5 May 2004; accepted 13 December 2004; published online 7 March 2005)

Germanium combined with high-κ dielectrics has recently been put forth by the semiconductor industry as potential replacement for planar silicon transistors, which are unlikely to accommodate the severe scaling requirements for sub-45-nm generations. Therefore, we have studied the atomic layer deposition (ALD) of HfO_2 high-κ dielectric layers on HF-cleaned Ge substrates. In this contribution, we describe the HfO_2 growth characteristics, HfO_2 bulk properties, and Ge interface. Substrate-enhanced HfO_2 growth occurs: the growth per cycle is larger in the first reaction cycles than the steady growth per cycle of 0.04 nm. The enhanced growth goes together with island growth, indicating that more than a monolayer coverage of HfO_2 is required for a closed film. A closed HfO_2 layer is achieved after depositing 4–5 HfO_2 monolayers, corresponding to about 25 ALD reaction cycles. Cross-sectional transmission electron microscopy images show that HfO_2 layers thinner than 3 nm are amorphous as deposited, while local epitaxial crystallization has occurred in thicker HfO_2 films. Other HfO_2 bulk properties are similar for Ge and Si substrates. According to this physical characterization study, HfO_2 can be used in Ge-based devices as a gate oxide with physical thickness scaled down to 1.6 nm. © *2005 American Institute of Physics*. [DOI: 10.1063/1.1856221]

I. INTRODUCTION

Germanium is a high-performance device material due to its narrow band gap, high mobility and low dopant activation temperatures. It has recently been put forth by the semiconductor industry as a potential replacement for planar silicon, which is unlikely to accommodate the severe scaling requirements for sub-45-nm transistor generations. However, a major technological drawback to the use of Ge is the difficulty in growing an insulating oxide comparable to SiO_2 in Si technology. Deposited high-κ materials may provide a solution for the gate dielectric of Ge-based transistors. Indeed, the successful use of a ZrO_2 dielectric film in Ge field-effect transistors (FETs) has recently been demonstrated.[1] The low-field mobility for the Ge/ZrO_2 FETs was twice that of Si/SiO_2 FETs.[1]

High-performance devices in the sub-45-nm technology mode should reach the equivalent oxide thickness (EOT) targets below 0.8 nm. For ZrO_2 and HfO_2 dielectrics with a k value of 20–25, this means that films thinner than 4 nm should be deposited. Atomic layer deposition (ALD) is a suitable technique to deposit uniform films in the nanometer thickness range.[2,3] In order to function as a gate dielectric, the layer should also be smooth and contain no holes. As the ALD growth behavior can depend on the substrate,[4–8] it is important to investigate and compare the growth characteristics and morphology of the dielectric films on the specific substrates. At least two ALD growth characteristics are affected by the substrate. A first growth characteristic is the *growth per cycle* or growth rate, defined as the total amount of material deposited per reaction cycle.[6] The growth per cycle can be expressed as thickness increment (nm) or as increase of areal density (number of atoms/nm^2).[6] A second growth characteristic influenced by the substrate is the *growth mode*,[9] which refers to the way the deposited material is arranged on the substrate; the material can be deposited as islands, or in a more favorable case as a closed two-dimensional layer.

For the ALD of HfO_2 on Si substrates, using $HfCl_4$ and H_2O precursors, both growth per cycle and growth mode have been investigated for different surface preparations.[4,8,10–15] The growth per cycle can accurately be determined by means of a Rutherford backscattering spectroscopy (RBS) as the number of Hf atoms/nm^2. The growth per cycle as thickness can be obtained from the RBS Hf coverage assuming a value for the HfO_2 density,[6] or from ellipsometry if the layers are thicker than about 10 nm.[16,17]

[a] Also at K.U. Leuven, INSYS, Kasteelpark Arenberg, B-3001 Leuven, Belgium.
[b] Electronic mail: matty.caymax@imec.be

 © 2005 American Institute of Physics

Downloaded 16 Sep 2008 to 129.100.41.190. Redistribution subject to AIP license or copyright; see http://jap.aip.org/jap/copyright.jsp

On the other hand, the experimental determination of the growth mode is less straightforward. Essentially, we want to monitor the composition of the top surface of the sample and observe how fast the substrate intensity decreases as a function of the Hf coverage. Therefore, very surface sensitive techniques, such as low-energy ion scattering (LEIS) or time-of-flight secondary-ion-mass spectrometry (TOFSIMS) should be used. The combination of RBS and TOFSIMS has shown that the growth per cycle dependence on the substrate can give a first indication of the growth mode. Strong inhibition effects in the first ALD cycles have been associated with islandlike morphology and poor electrical properties of the dielectric layer.[4,8,11,15,18] Growth inhibition is very pronounced on hydrogen- terminated Si substrates and may be related to the low reactivity of the $HfCl_4$ precursor with Si–H bonds. The introduction of more reactive Si–OH groups, for example, by chemical oxidation[4] or by remote plasma treatments,[13] leads to a more constant growth per cycle and a more two-dimensional growth mode. LEIS has demonstrated HfO_2 layer closure after ten reaction cycles for ALD on chemical oxide substrates.[12]

In this contribution, we investigate the ALD of HfO_2 on Ge substrates by means of several complementary analysis techniques. Both growth per cycle and growth mode are studied using RBS, TOFSIMS, and LEIS. The Ge interface will be particularly important with respect to device performance. Therefore, the Ge interface is also investigated by means of x-ray photoelectron spectroscopy (XPS) and medium energy ion scattering (MEIS). Cross-sectional transmission electron microscopy (TEM), x-ray diffraction (XRD), and TOFSIMS depth profiling further characterize the HfO_2 layer on Ge substrates.

II. EXPERIMENTAL DETAILS

A. HfO_2 layer growth

Prior to deposition, 100-mm Ge(100) substrates were cleaned for 5 min in a 2% HF solution, rinsed in de-ionized water, and dried in clean room air. Both Ge(100) and miscut Ge(100) substrates were used. The miscut was 5.7° towards (111). The results for miscut Ge(100) were not different from the results for Ge(100). HfO_2 was deposited in an ASM ALCVD™ Pulsar 2000 reactor, integrated on a Polygon™ 8200 platform.[19] All depositions were performed at 300 °C with $HfCl_4$ and H_2O precursors. The pressure in the reactor was 1 Torr. The cycle numbers ranged between 1 and 300. The pulse and purge times were optimized for HfO_2 films grown in tens to hundreds of ALD reaction cycles. The optimized process gave uniform HfO_2 films over the 100-mm Ge wafers. Reactant doses below that needed for saturation caused a sharp thickness decrease at the back end of the wafer. Small changes in the pulse and purge times did not affect the amount of material deposited. Uniform film thickness and low sensitivity towards pulse and purge times indicated that surface saturation was obtained and ALD conditions prevailed.

B. XPS

Ge/HfO_2 samples were analyzed by XPS after several weeks of air exposure. XPS measurements were performed in a Quantum 2000 from Phi (Q1) using a monochromatic Al K_α radiation in a high-power mode (100 W, measuring spot 100 μ, scanned over 1400×500 μ^2). The angle between the axis of the analyzer and the sample surface was 90°. The amount of C was found to be ~10 at. %, which is a normal contamination level for samples stored in ambient air. The Ge2*p* line, corresponding to a kinetic energy of 260 eV, was detectable only for HfO_2 samples of less than 60 cycles. Thicker HfO_2 layers attenuate the Ge2*p* signal too much. Due to a strong overlap between the O2*s* (from HfO_2) and the Ge3*d* peak, this region could not be used to analyze the oxidation of the Ge interface. The Ge3*s* lines gave chemical information about the bottom interface. Standard sensitivity factors were used to convert peak areas to atomic concentrations. The thickness of the GeO_2 and HfO_2 layers was estimated by means of a three-layer model calculation.[20] The escape mean free paths of the photoelectrons was calculated using the Tanuma–Powell–Penn (TPP2) formula.[21]

The HF-cleaned Ge substrate was also characterized by XPS. The air exposure between cleaning and XPS measurement was limited to less than 15 min. The Ge3*d* lines were analyzed.

C. RBS

RBS was performed in a RBS400 Endstation (Charles Evans and Associates) which is installed around a 6SDH-12MV tandem (National Electrostatics Corporation). The measurements were performed with a 1-MeV He^+ beam in a rotating random mode. The scatter angle was 168°. The accumulation dose was 20 μC. Beam current was limited to 5 nA to avoid pile up in the electronics. A beamchopper was used for normalization. The RUMP simulation code was applied to calculate the areal density of Hf (number of $atoms/cm^2$).

D. LEIS

LEIS measurements were performed with 3-keV $^4He^+$ and $^{20}Ne^+$. First a $^4He^+$ measurement was performed to get a general impression of the surface composition, using an ion dose of 2.1×10^{13} $ions/cm^2$ to measure one spectrum. Measurements with 3-keV $^{20}Ne^+$ were performed directly after the $^4He^+$ measurements using an ion dose of 1.1×10^{13} $ions/cm^2$. For each sample the analysis was based upon an average of three spectra to obtain adequate statistics. There was a linear dependency between the Hf and Ge intensities, which allows a reliable determination of maximum Hf and Ge intensities by extrapolation. The surface fractions of Hf and Ge were calculated by dividing the Hf and Ge intensity by their maximum intensities.

Cleaning the sample surface prior to LEIS analysis is inevitable as organics, adsorbed during air exposure between sample preparation and LEIS analysis, diminish the surface spectrum intensity. Two different cleaning methods prior to LEIS analysis were used: low-energy atomic oxidation and calcination. Low-energy atomic oxidation was performed at

Downloaded 16 Sep 2008 to 129.100.41.190. Redistribution subject to AIP license or copyright; see http://jap.aip.org/jap/copyright.jsp

room temperature with 10^{-4}-mbar oxygen pressure. The minimum time needed to obtain a clean surface by atomic oxidation was determined for a sample consisting of 5-cycles HfO_2 deposited on a HF-cleaned Ge. An increase of the complete spectrum intensity was observed with increasing oxidation time, indicating a decreasing content of organics. Extrapolation of the results after 0, 3, 6, and 9-min oxidation indicated that 15 min was sufficient to obtain a clean surface. In a second cleaning method, samples were first calcined for 20 min at 300 °C using an oxygen pressure of 200 mbar. After calcination, samples were oxidized using atomic oxygen. Subsequent atomic oxidation treatments did not change the LEIS spectrum, suggesting a fully cleaned surface after calcination. However, the HfO_2 peak area was systematically lower after calcination than after atomic oxidation. This indicates that the surface was altered during calcination: either HfO_2 has clustered or $Ge(O_2)$ has segregated to the surface. Only LEIS results after the first cleaning method, atomic oxidation only, will therefore be used for analysis of the HfO_2 growth mode.

E. TOFSIMS

All TOFSIMS measurements were performed using an Ion TOF-IV instrument using a 10-keV Ar^+ analysis ion beam. Normalized intensities were calculated by dividing the Hf and Ge intensity by the signal measured on a pure HfO_2 or Ge surface. For the depth profiles, a dual beam setup with a 500-eV Ar^+ ion beam was used.

F. MEIS

The MEIS instrument (High Voltage Engineering B.V., Amersfoort, the Netherlands) has been described in detail elsewhere.[22,23] Protons with an energy of 98.80 ± 0.08 keV were used. Backscattered ion energies were analyzed with a high-energy-resolution toroidal electrostatic detector[24,25] ($\Delta E/E \sim 0.1\%$). Depth profiles of the elements were obtained from simulations of the measured backscattered ion energy distribution assuming that the film densities are known or can be extrapolated from known data. The scattering geometry used had the incident beam aligned in the [001] direction, deviating ~5.7° from macroscopic surface normal, due to the miscut of the Ge substrate wafer. Therefore, the data were acquired at a scattering angle of 130.7°. Prior to MEIS analysis, the samples were exposed to air for several days. Only minor top surface carbon contamination was detected.

G. TEM

Cross-sectional TEM specimens were prepared by conventional ion milling and observed in Jeol 200CX and Philips CM30 TEMs at 200 and 300 kV, respectively.

H. XRD

A high-temperature grazing incidence x-ray diffraction (HT-GI-XRD) was performed with a θ-θ XRD diffractometer (3003 TT Seifert, Ahrensburg, Germany) using a Cu $K\alpha$ source radiation and an incidence angle of 3°. The diffractometer is equipped with a parabolic multilayer mirror for parallel beam optics and a furnace for *in situ* high-temperature XRD tests. The sample was heated from room temperature to a test temperature, at which a scan in the 2θ range from 20 to 40 takes about 30 min. After the scan, the sample was heated to a higher temperature for a new scan with the same schedule.

TABLE I. XPS and MEIS GeO_x thickness (nm). * not measured.

Sample	GeO_x thickness (nm)	
	XPS	MEIS
HF-cleaned Ge	0.2–0.3	*
HF-cleaned Ge+30-cycles HfO_2	*	0.3
HF-cleaned Ge+40-cycles HfO_2	0.3	*
HF-cleaned Ge+60-cycles HfO_2	0.4	0.3
HF-cleaned Ge+80-cycles HfO_2	0.4	*

III. RESULTS

A. XPS

First, XPS measurements were performed to characterize the uncleaned and HF-cleaned Ge substrate. The Ge3*d* lines (spectrum not shown) were measured at binding energy between 28 and 35 eV and were separated into substrate Ge and oxidized Ge. After HF clean, the binding energy of the oxidized Ge peak significantly reduced in intensity and shifted from 33 to 32 eV. This indicates that the native oxide on the uncleaned Ge wafer, consisting mainly of GeO_2, was etched during HF clean. Only a limited amount of suboxide (0.2–0.3 nm) was present after the HF clean (Table I).

Second, XPS was used to characterize the Ge interface of samples with 40, 60, and 80 cycles of HfO_2. The Ge3*s* were separated into substrate Ge (at 182.2 eV) and interfacial GeO_2 (at 184.9 eV) [Fig. 1(a)]. As expected, the intensity of the Ge signal decreased with increasing Hf coverage. The thickness of the GeO_2 interfacial layer, as deduced from a three-layer model, was small (0.3 nm) (Table I). The Hf4*f* peaks consisted of one single doublet with a peak position at 17.2 eV [Fig. 1(b)]. No indications for metallic Hf or Hf suboxides were observed.

B. RBS

The RBS Hf content as a function of the number of ALD cycles is shown in Fig. 2. The growth per cycle in the first ten ALD reaction cycles is shown in Fig. 3. The ALD growth was enhanced by the Ge substrate; the growth per cycle was higher in the first reaction cycles than in the steady regime. The amount of Hf deposited in the first reaction cycle is 7.6 Hf/nm^{-2}. This corresponds to almost one monolayer of HfO_2 (9.15 Hf/nm^{-2}), as calculated from the bulk density of HfO_2 (9.68 $g\,cm^{-3}$).[6,26] Within few cycles, the growth per cycle decreased to a steady value of about 1.1 $Hf\,nm^{-2}$, or 0.040 nm assuming the bulk density. Thus, the steady growth is similar as the case of HfO_2 growth on Si substrates.[4,15]

Downloaded 16 Sep 2008 to 129.100.41.190. Redistribution subject to AIP license or copyright; see http://jap.aip.org/jap/copyright.jsp

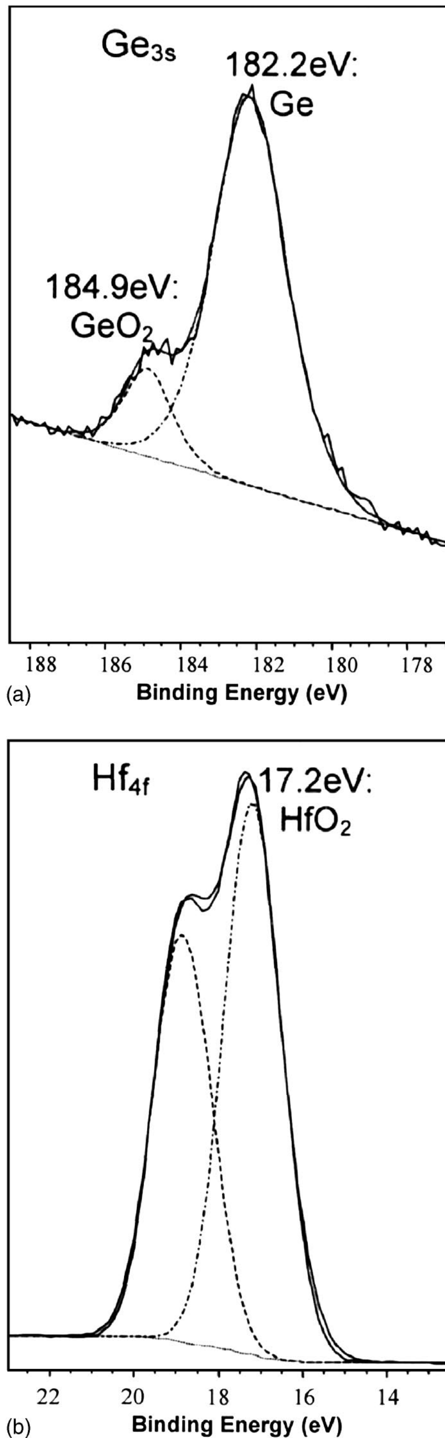

FIG. 1. XPS spectra for (a) Ge3*s* and (b) Hf4*f* for a sample with 80-cycles HfO_2 deposited on HF-cleaned Ge.

C. LEIS

Figures 4(a) and 4(b), respectively, show the $^4He^+$ and $^{20}Ne^+$ LEIS spectra measured after atomic oxidation on samples with different number of HfO_2 cycles. Peaks of O, Ge, and Hf were clearly visible. No other elements were observed. The surface of the pure Ge wafer (0 cycles) was oxidized, as shown by the O peak in the LEIS spectrum [Fig. 4(a)]. With increasing number of cycles, the Ge peak decreased and the Hf peak increased. After 25 cycles, the Ge surface was fully covered by HfO_2, as shown by the absence of a Ge peak in the $^{20}Ne^+$ spectrum [Fig. 4(b)]. From this point, the Hf peak in the $^4He^+$ spectrum substantially broadens to the low-energy side. Asymmetric broadening originates from ion scattering of Hf atoms below the surface.[27]

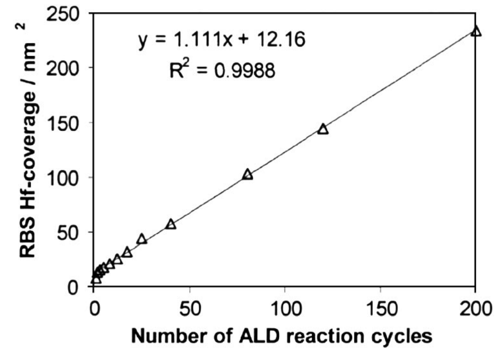

FIG. 2. Hf coverage measured by RBS as a function of the number of ALD reaction cycles on HF-cleaned Ge substrates.

The HfO_2 and Ge surface fractions, calculated by normalizing the LEIS Hf and Ge signals, are shown in Fig. 5. The HfO_2 surface fraction increased and the Ge surface fraction decreased with the number of ALD reaction cycles, as expected. After 25 cycles; the HfO_2 film covers the surface completely.

D. TOFSIMS

Figure 6 shows the evolution of the normalized Hf and Ge intensities at the top surface, as measured by TOFSIMS. Similarly as in LEIS, the HfO_2 intensity increased and the Ge intensity decreased with the number of cycles. The TOFSIMS Hf signal follows the same trend as LEIS, with saturation around 25 reaction cycles.

TOFSIMS was also used to achieve a depth profile of the Hf, Cl, and Ge intensities (Fig. 7). No significant amount of Ge was observed in the HfO_2 bulk. The shape of the Cl profile for HfO_2 deposition on Hf-cleaned Ge is similar to that for HfO_2 deposited on Si substrates,[28] with a Cl peak at the bottom HfO_2 interface.

E. MEIS

MEIS was used to estimate film composition and interfacial oxide thickness. Figure 8 shows a proton backscatter-

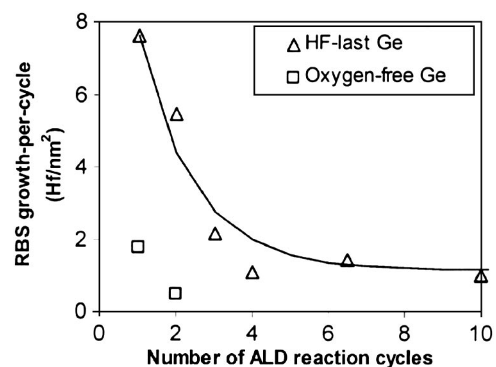

FIG. 3. Growth per cycle from RBS in the first ten ALD reaction cycles for HF-cleaned Ge and oxygen-free Ge. The black line shows a trend line through the RBS data. This trend line is used for growth mode simulations.

Downloaded 16 Sep 2008 to 129.100.41.190. Redistribution subject to AIP license or copyright; see http://jap.aip.org/jap/copyright.jsp

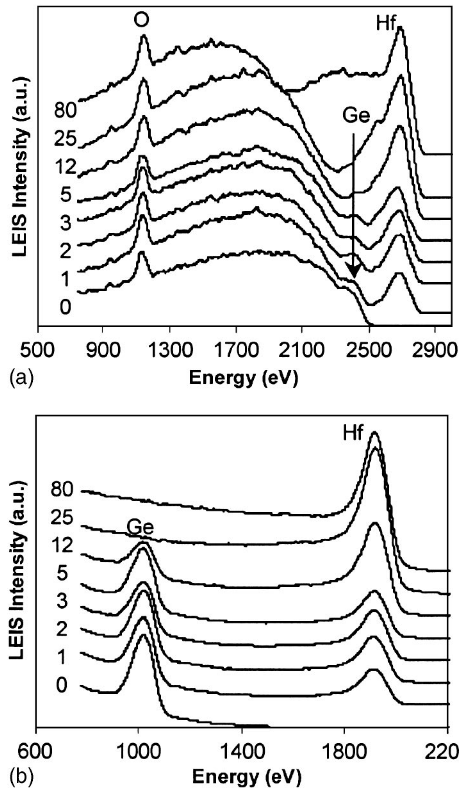

FIG. 4. LEIS spectra after atomic oxidation measured with (a) 3-keV $^{4}He^{+}$ ions and (b) 3-keV $^{20}Ne^{+}$ ions. The number of ALD reaction cycles is indicated in the figure.

ing energy spectrum from an as-deposited 3-nm-thick HfO_2 film. Both 3- and 6-nm HfO_2 spectra can be fitted with very thin (0.3 nm) GeO_x interfacial oxides (Table I). The $HfO_2/GeO_2/Ge$ interfaces are likely to be sharp, the position of the Ge peak indicating that there is not much Hf–Ge–O intermixing. In addition, Cl concentrations of about 10^{15} atoms/cm^2 were detected close to the Ge interface, attributed to the use of the $HfCl_4$ precursor in the ALD process. Probably, this Cl is distributed in several monolayers located close to the Ge interface. MEIS angular distribution profiles show no evidence for crystallinity, both 3- and 6-nm HfO_2 films appearing to be amorphous.

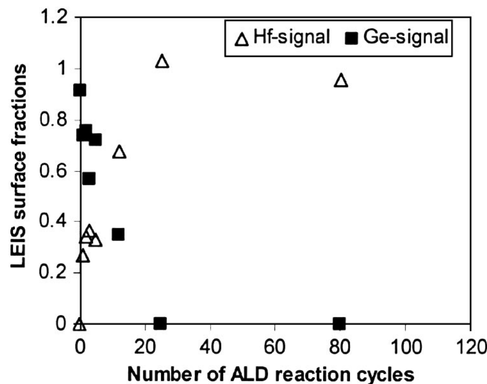

FIG. 5. LEIS surface fractions of Hf and Ge as a function of the ALD cycle number for atomic oxygen cleaned samples. The Ge surface fraction of the sample without HfO_2 is not exactly equal to 1, as the maximum Ge intensity was estimated from extrapolation (Sec. II D).

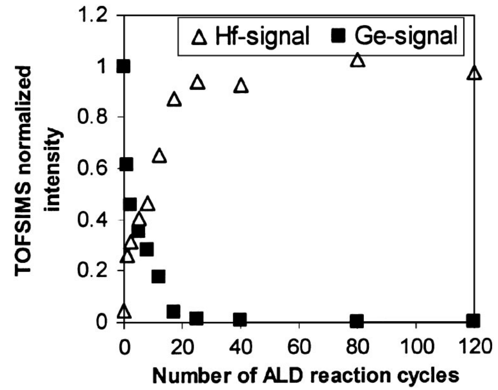

FIG. 6. Evolution of the normalized TOFSIMS Hf and Ge intensity as a function of the number of ALD cycles.

F. TEM

Cross-sectional TEM images of samples with 12-, 40-, and 200-cycles HfO_2 deposited on an HF-cleaned Ge substrate are shown in Fig. 9. The Ge interface was smooth. A bright contrast layer was observed at this interface. This contrast is most probably due to the presence of a thin interfacial oxide layer, as indicated by XPS and MEIS. The thin HfO_2 layers both were amorphous as deposited. The 200-cycles HfO_2 layer was 9.0 nm thick and polycrystalline. Some crystals were formed in epitaxy with the Ge substrate; one can see the continuation of the (111) Ge crystallographic planes through the interface.

The HfO_2 thickness deduced from TEM is shown in Table II. HfO_2 densities were calculated for the three samples by combining the TEM HfO_2 thickness and RBS Hf coverage.

G. XRD

XRD measurements were performed on as-deposited samples with 100-, 200-, and 300-cycles of HfO_2, which

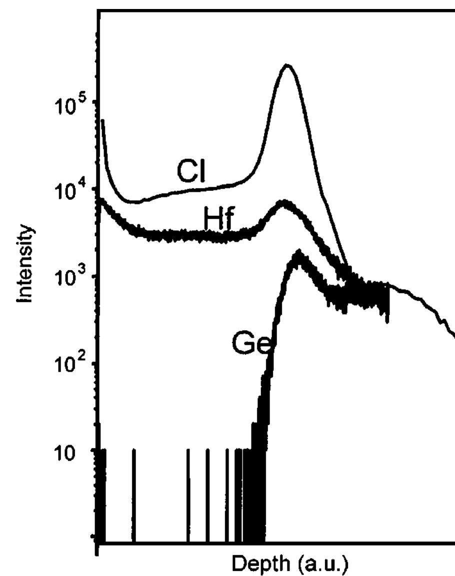

FIG. 7. TOFSIMS Hf, Cl, and Ge depth profiles for a 200-cycles HfO_2 layer (9 nm) deposited on an HF-cleaned Ge substrate. The Cl profile was measured in the negative ion polarity while the Hf and Ge profiles were measured in the positive ion polarity. The intensities can thus not be directly compared.

Downloaded 16 Sep 2008 to 129.100.41.190. Redistribution subject to AIP license or copyright; see http://jap.aip.org/jap/copyright.jsp

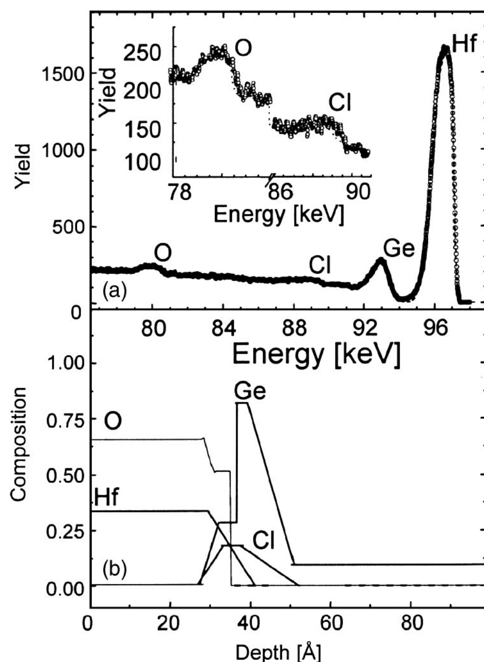

FIG. 8. (a) Experimental MEIS spectrum (dots) and calculated H^+ yield (solid line) for a 60-cycles HfO_2 layer (3 nm) deposited on HF-cleaned Ge. The oxygen and chlorine peaks are shown enlarged in the insert. (b) The Hf, Ge, O, and Cl depth profiles used for the calculated H^+ yields in (a).

correspond to 5-, 9-, and 14-nm, respectively. Figure 10 shows the results for 14-nm HfO_2. The as-deposited layer is partially crystalline and is composed of 10 vol % cubic, 10 vol % monoclinic, and 80 vol % amorphous phase. At 400 °C, a fully crystalline layer forms. With the increase of temperature, the cubic phase, which is metastable in the temperature range of the test, transforms into a monoclinic phase. A similar phase transformation occurs for HfO_2 on Si

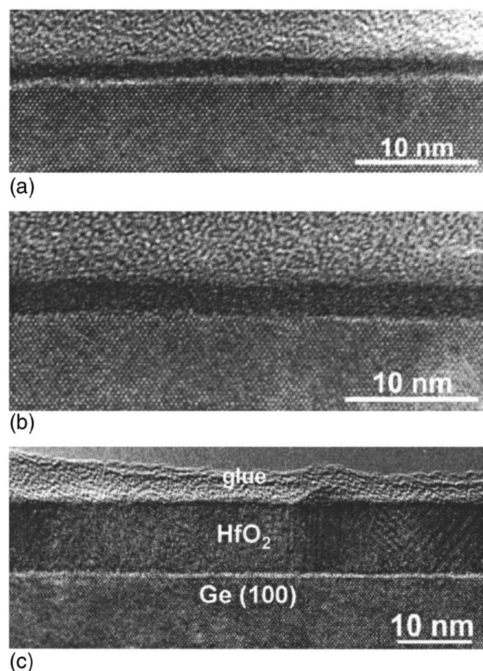

FIG. 9. Cross-sectional TEM images of a (a) 12-cycles, (b) 40-cycles, and (c) 200-cycles HfO_2 layer deposited on a HF-cleaned Ge(100) substrate.

TABLE II. Density of HfO_2 layers deduced from the TEM thickness (Fig. 9) and the RBS Hf coverage (Fig. 2).

Number of ALD cycles	TEM thickness (nm)	HfO_2 density (10^{22} HfO_2/cm^3)	% of HfO_2 bulk density
12	1.6	1.59	58
40	2.6	2.22	80
200	9.0	2.69	97

substrates.[29] At 800 °C, only a very small amount of cubic phase remains. The spectra shown in Fig. 10 reveal $m(200)$ and (002) textures, or the intensities of the peaks are higher than in powder diffraction. This indicates the epitaxial orientation of the crystallites.

XRD indicated that thinner HfO_2 layers (5 and 9 nm) were amorphous as deposited, and crystallize at a temperature between 300 and 400 °C. The phase transformation from cubic to monoclinic is also observed.

IV. DISCUSSION

A. Reactive sites at the Ge substrate

The chemical composition of the substrate can influence both growth per cycle and growth mode of the atomic layer deposition. Therefore, we have characterized the Ge substrate after HF clean with XPS. A small amount of suboxide remains present on Ge after HF clean (Table I). Prior to HfO_2 deposition, this substrate is conditioned in the ALD reactor at 300 °C in 1 Torr of N_2. At this temperature, H starts to desorb from the Ge(100) substrate.[30,31] High-resolution electron energy-loss spectroscopic (HREELS) studies have shown that the dihydride and monohydride coverage decreases to zero at 300 and 380 °C, respectively.[32] It has been shown that coadsorbed O creates little perturbation to the H desorption kinetics of Ge.[30] Above 300 °C, O is proposed to be present in the form of a bridge-bonded species,[30] although

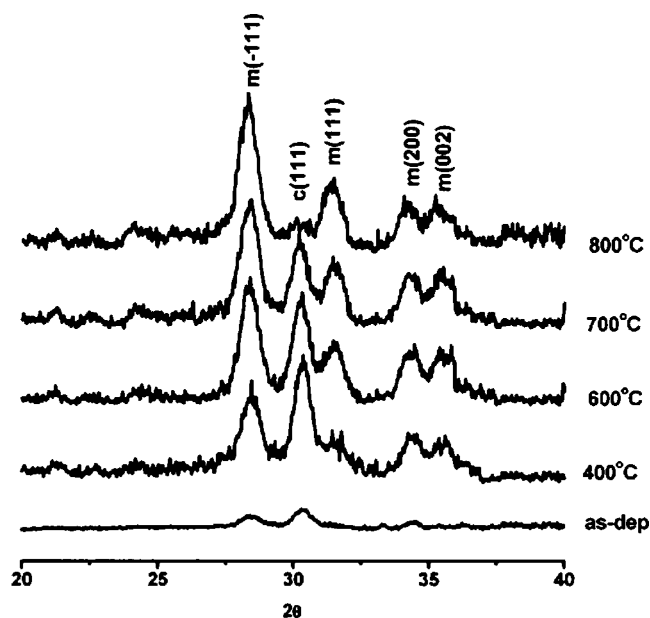

FIG. 10. XRD spectra as a function of temperature for a 300-cycles HfO_2 layer (14 nm) deposited on HF-cleaned Ge.

Downloaded 16 Sep 2008 to 129.100.41.190. Redistribution subject to AIP license or copyright; see http://jap.aip.org/jap/copyright.jsp

OH groups may also be present. Thus, monohydrides, oxygen bridges as well as OH groups could be present at the Ge substrate before ALD.

For HF-cleaned Si(100), on the other hand, no significant amount of oxide is present.[33] Both mono-, di-, and trihydrides are present at the HfO_2 ALD process temperature, as H desorption occurs only at temperatures above 500 °C.[33,34] Si–H is known to be a very low-activity site for ALD with metal chloride precursors.

Thus, the active sites for ALD on HF-cleaned Ge probably are OH groups, possibly also the Ge–O–Ge bridge configuration, probably not Ge–H. As the reactive sites at HF-cleaned Ge and Si substrates clearly are very different, we can expect a different growth behavior on HF-cleaned Ge and Si substrates. This will indeed be shown in the following paragraphs.

B. Analysis of the HfO_2 growth mode

The normalized intensities of the substrate and the deposited HfO_2 layer (obtained from LEIS and TOFSIMS) give information about the growth mode when they are combined with the total amount of HfO_2 deposited (as measured by RBS). In the *two-dimensional growth mode* (also called layer-by-layer growth and Frank van der Merwe growth), the surface fraction of the substrate first decreases linearly with the amount of material deposited. From the point where one HfO_2 monolayer (9.15 Hf/nm^{-2}) is present, it is zero. On the other hand, an approximately exponential decay of the substrate surface fraction is expected in the *random deposition mode*.[7,35] In this growth mode, all surface sites have the same probability of deposition. If the substrate intensity decay is even slower than in the random deposition mode, island growth is prevailing.[36] We will compare LEIS and TOFSIMS results with the theoretical models in order to determine the growth mode.

The interpretation of LEIS results is straightforward because the measured intensity comes from the first atomic layer and, as such, directly gives the surface fraction. Theoretical surface fraction curves for two-dimensional and random deposition were calculated, as described in Ref. 7, using the growth per cycle curve shown in Fig. 3. The LEIS surface fractions for HfO_2 growth on HF-cleaned Ge deviate significantly from the theoretical surface fraction curves, both for two-dimensional and random deposition [Fig. 11]. According to the two-dimensional growth, the HfO_2 layer should be closed already at about 9.15 Hf/nm^{-2}, much earlier than observed by LEIS, about 40 nm^{-2}. The closure point measured with LEIS for HfO_2 deposition on HF-cleaned Ge is similar as expected on the basis of random deposition. However, before closure we observe a significant deviation between the measured and calculated curves; LEIS systematically shows higher Ge and lower HfO_2 surface fractions. This demonstrates that island growth (Volmer–Weber growth) takes place.[7] Another possibility is that Hf mixes with Ge, forming a $HfGeO_x$ layer.

The interpretation of the TOFSIMS substrate intensities is more complicated than LEIS, as not only the outermost

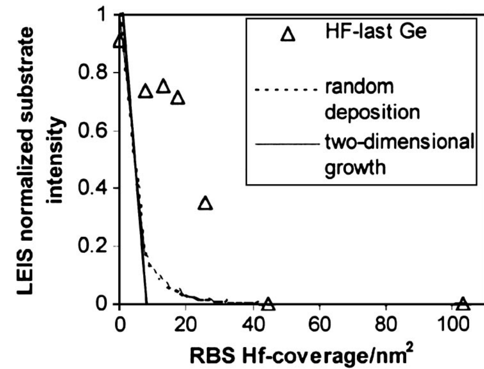

FIG. 11. Normalized LEIS Ge intensity (corresponding to surface fractions) as a function of the RBS Hf content, as compared to two-dimensional growth and random deposition.

surface but the first few atomic layers can determine the TOFSIMS intensity. An exponential decay of the substrate intensity is often observed[4,18]

$$I/I_0 = \exp(-t/\lambda).$$

Here, t is the film thickness. λ can be considered as a parameter that qualitatively describes how fast the layer closes. For HfO_2 growth on Si chemical oxide, which is close to two dimensional, the TOFSIMS Si signal decays exponentially with $\lambda \approx 0.2$ nm.[4] This decay curve is shown in Fig. 12 together with the TOFSIMS Ge decay curve for HfO_2 deposition on HF-cleaned Ge. Up to 12 ALD cycles, the Ge intensity decays much slower as compared to the two-dimensional reference. The data points can be fitted with an exponential function with $\lambda = 0.6$ nm. This high λ value again points to island growth. The TOFSIMS decay of the Ge substrate signal accelerates after 12 ALD reaction cycles (Figs. 6 and 12).

Although LEIS and TOFSIMS both suggest the formation of islands, islands are not directly visible with TEM. For 12-cycles HfO_2, LEIS shows that only 60% of the substrate is covered by HfO_2. However, the HfO_2 layer visible on the cross-sectional TEM image appears to be closed and rather smooth [Fig. 9(a)]. The islands and voids between islands are expected to be of much smaller dimensions than the thickness of the TEM cross section (50–100 nm). Therefore, it is not possible to distinguish them individually in the cross-

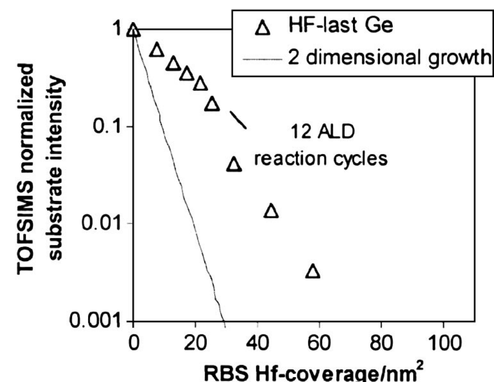

FIG. 12. Experimental TOFSIMS decay of the Ge signal as compared to the theoretical decay for two-dimensional growth [$I/I_0 = \exp(-t/\lambda)$ with $\lambda = 0.2$ nm].

Downloaded 16 Sep 2008 to 129.100.41.190. Redistribution subject to AIP license or copyright; see http://jap.aip.org/jap/copyright.jsp

section view due to the dark contrast of HfO_2. Plan view TEM, on the other hand, gives a "top view" of the sample. However, plan view TEM (not shown) also could not confirm the presence of the HfO_2 islands because the thin HfO_2 layer gave a too weak contrast.

The islandlike growth on HF-cleaned Ge must be distinguished from the island growth, for example, on HF-cleaned Si. First, it goes together with the growth enhancement instead of the growth inhibition observed on HF-cleaned Si.[4,8,10] Second, the HfO_2 layer closure on HF-cleaned Ge is faster as compared to HF-cleaned Si; the HfO_2 layer on Ge closes after about 1.6 nm, while for Si more than 4 nm must be deposited.[37] The faster layer closure can indicate that there are more nucleation sites at the HF-cleaned Ge substrate (e.g., OH, see Sec. IV A), as compared to HF-cleaned Si. A higher island density can then be expected, resulting in faster layer closure.

C. Analysis of growth enhancement

Growth enhancement in the first reaction cycles is not common for ALD processes, although in some cases it has been observed.[12,14,38,39] The Ge surface is very smooth, so the high growth per cycle cannot be attributed to surface roughness or even a microporous structure such as, e.g., in the ALD growth of Al_2O_3 on SILK.[38]

The possible reactions involved in the chemisorption of $HfCl_4$ on the Ge substrate can be analyzed by means of a recent model of growth per cycle in ALD.[6] The model is based on the mass balance of chemisorption and assumes a two-dimensional arrangement of the adsorbed ligands. The amount of Hf adsorbed in the first reaction cycles is directly obtained from the growth per cycle as 7.6 nm^{-2} [Fig. 3]. During the $HfCl_4$ reaction, each Hf atom brings along four Cl ligands (using the $HfCl_4$ precursor). Thus, according to mass balance, about 30 Cl ligands nm^{-2} arrive to the surface. The maximum number of Cl ligands remaining on a flat surface when steric hindrance prevails can be estimated from the van der Waals radius of Cl [0.175 nm (Ref. 40) as 9.4 nm^{-2}].[6] Therefore, according to the growth per cycle model, at least $(30-9.4)\approx 21$ Cl ligands nm^{-2} must have been removed from the surface. The typical mechanism for removing Cl ligands is ligand exchange in which Cl is released as HCl

$$m\mathrm{OH}^* + \mathrm{MCl}_n \rightarrow m\mathrm{OMCl}^*_{n-m} + m\mathrm{HCl},$$

where the asterisk denotes a surface species. This would require the presence of at least 21 OH groups per nm^2 on the Ge surface before the $HfCl_4$ reaction. This is much more than allowed by steric hindrance, considering the van der Waals radius of 0.14 nm for OH. Thus, the growth per cycle seems to be higher than allowed by steric hindrance in the model.[6]

The assumption that a two-dimensional layer of adsorbed species is formed[6] may not be valid in this case. Indeed, the combination of LEIS and RBS indicates that, in the first reaction cycle, HfO_2 is not present as a flat monolayer but more probably as supermonolayer-high islands. Spreading out 7.6/Hf nm^{-2} over the substrate as a monolayer would give a surface fraction of 83%. However, LEIS shows that only 28% ±5% of the Ge substrate is covered after the first reaction cycle. This indicates the presence of islands of on average three monolayers high in the first reaction cycle. Such islands could indeed allow a much higher Cl coverage as compared to a flat surface due to a larger effective area.[41]

The formation of supermonolayer-high islands shows that the HfO_2 growth on Ge is nonideal, because the height of the islands after one reaction cycle should not exceed one monolayer. One possible explanation would be the occurrence of gas phase reactions between Hf- and O-containing compounds. One obvious O source is the H_2O precursor that could linger around in the gas phase during the subsequent $HfCl_4$ pulse. We have investigated the separation of the precursor pulses by considering various purge times between these pulses up to 10 s. The amount of HfO_2 deposited in the first reaction cycle was found to be independent on the purge time, suggesting a clear separation between $HfCl_4$ and H_2O pulses. Another source of O could be OH on the Ge surface (as known from XPS measurements) that could be transported into the gas phase according to the following reaction:

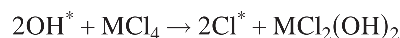

$$2\mathrm{OH}^* + \mathrm{MCl}_4 \rightarrow 2\mathrm{Cl}^* + \mathrm{MCl}_2(\mathrm{OH})_2$$

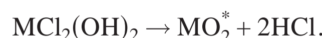

$$\mathrm{MCl}_2(\mathrm{OH})_2 \rightarrow \mathrm{MO}_2^* + 2\mathrm{HCl}.$$

This process is often referred to as agglomeration.[42,43] This agglomeration process may occur when metal halide precursors are used, for example, for the $TiCl_4/H_2O$ TiO_2 and $ZrCl_4/H_2O$ ZrO_2 ALD processes.[44–49] The transport of oxygen from the substrate to the growing metal oxide particle might be explained by an intermediate $MCl_2(OH)_2$ species, moving OH groups from the substrate to the formed metal chloride surface species. No clear evidence has been presented for agglomeration reactions in HfO_2 ALD on Si substrates. However, agglomeration could occur more easily on Ge substrates, as the Ge–O bond is weaker than the Si–O bond, facilitating the release of O necessary for the formation of the agglomerates.

Some support for the agglomeration mechanism comes from the growth studies of HfO_2 on an O-free Ge substrate. The XPS spectrum clearly demonstrated that no GeO_2 or suboxide was present on this substrate before HfO_2 deposition. The growth per cycle for HfO_2 deposition on O-free Ge was significantly lower as compared to HF-cleaned Ge substrates (Fig. 3), indicating that the growth enhancement is related to the presence of oxygen at the Ge substrate. Furthermore, agglomeration has usually been associated with chlorination of the substrate. According to MEIS and TOF-SIMS, there was indeed a significant amount of Cl present close to the Ge interface for deposition on HF-cleaned Ge. TOFSIMS indeed indicates that the Cl peak at the bottom interface is higher for HfO_2 deposition on Ge substrates, as compared to Si substrates (see also Sec. IV D).

D. HfO_2 bulk properties on Ge substrates

1. Density

The density of the HfO_2 layers (Table II) depends on the layer thickness. A similar dependence was also observed for ALD HfO_2 on Si substrates[17,50] and for metal-organic

Downloaded 16 Sep 2008 to 129.100.41.190. Redistribution subject to AIP license or copyright; see http://jap.aip.org/jap/copyright.jsp

chemical-vapor deposition (MOCVD) HfO_2 on Si substrates.[50] The low density of the thinnest layers could reflect their island morphology. For closed HfO_2 layers on Ge substrates, a density of more than 80% of the bulk density is obtained. This is in agreement with the density of ALD HfO_2 deposited on Si substrates with similar thickness.[4,17]

2. Ge/Hf intermixing

TOFSIMS depth profiles (Fig. 7) indicate no significant concentration of Ge in the HfO_2 bulk, in contrast to what is observed, for example, for HfO_2 deposited by MOCVD on HF-cleaned Ge substrates.[51]

3. Impurities

Both TOFSIMS and MEIS show some Cl in the ALD HfO_2 films due to the use of the $HfCl_4$ precursor. TOFSIMS indicates a similar bulk Cl content for Ge and Si substrates. However, the Cl peak at the bottom interface is higher for Ge substrates. This could be due to substrate chlorination reactions associated with the agglomeration process. MEIS indicates a Cl content close to the Ge interface of about $10\ \mathrm{Cl/nm^2}$. As this Cl content corresponds to about one monolayer, the Cl is probably distributed in several monolayers located close to the Ge interface.

4. Crystallization behavior

Cross-sectional TEM, XRD, and MEIS show that thin HfO_2 layers (<9 nm) are amorphous as deposited. XRD shows that a 14-nm-thick HfO_2 layer is partially crystalline, with some HfO_2 grains oriented in epitaxy with the Ge substrate (Fig. 10). XRD and TEM disagree on the critical HfO_2 thickness at which crystallization starts to occur. With TEM, crystals are already observed in a 9-nm HfO_2 layer. On the other hand, XRD shows no diffraction peaks for a 9-nm HfO_2, but they appear for a 14-nm HfO_2 layer. The sensitivity of XRD is probably not sufficient to detect a limited amount of crystalline phase. Alternatively, the crystallites observed in a 9-nm layer by TEM might have grown in such an orientation that grazing incidence XRD cannot detect them.

The fact that thin films are amorphous implies that also thicker layers are amorphous in the first stages of the deposition process. As such, epitaxial crystallization occurs in a later stage of the ALD process, not during the ALD gas-substrate reactions itself. The presence of small amounts of O or Cl at the Ge interface and the lattice mismatch between the Ge and HfO_2 probably locally hinders full epitaxial crystallization of the HfO_2 film. Local epitaxial ZrO_2 crystals were also observed for a 5.5-nm ZrO_2 layer deposited by ALD on HF vapor-cleaned Ge(100) substrates[39] and for HfO_2 deposited by MOCVD on Ge.[51]

The crystallization behavior as a function of temperature, as studied by means of XRD, is similar for Ge and Si chemical oxide substrates.[29] A fully crystalline layer forms during a thermal treatment at low temperature. With the increase of temperature, the transformation from cubic to monoclinic phase is observed. The main difference for Ge and Si substrates is that no epitaxial crystallization was observed on Si.

E. The Ge interface

The interface between HfO_2 and the Ge channel will be particularly important in regard to device performance. First, the presence of low-quality Ge oxide or suboxide may degrade the electrical performance. Second, the thickness of the interfacial layer (with low-κ value) directly adds to the equivalent oxide thickness (EOT) of the high-κ stack. It should therefore be as thin as possible if subnanometer EOT targets are aimed for.

The cross-sectional TEM images (Fig. 9) show a smooth Ge interface with no obvious indication of an interfacial layer. XPS and MEIS investigations both indicate the presence of a thin (about 0.3 nm) oxide interfacial layer. Moreover, the XPS binding energy of the Ge3*s* lines indicates that the chemical composition of the interfacial layer is GeO_2.

The stability of the interfacial oxide layer during air exposure is important in case the gate is subsequently deposited *ex situ*. For nonclosed HfO_2 layers deposited on Ge, ellipsometer measurements show a thickness increase during air exposure due to interfacial oxide growth. LEIS also indicates that nonclosed HfO_2 layers on Ge are not stable during calcinations at 300 °C. For ZrO_2 and Al_2O_3 layers deposited on Si substrates, it has also been reported that interfacial oxide forms easily during air exposure when the high-κ layers are not fully closed.[37,52] Closed HfO_2 layers on Ge, on the other hand, are stable during air exposure.

V. CONCLUSIONS

We have demonstrated the atomic layer deposition of HfO_2 on HF-cleaned Ge substrates using the $HfCl_4$ and H_2O precursors. According to this physical characterization study, the physical thickness of HfO_2 dielectric layers grown on HF-cleaned Ge can be scaled down to about 1.6 nm. Optimization of the surface preparation resulting in a more two-dimensional growth mode may allow the further scaling of dielectrics layers to less than 1.6 nm. A second critical issue for the ultimate scaling of the Ge/high-κ stacks is the interfacial layer. A promising observation for HfO_2 stacks deposited on HF-cleaned Ge is that the bottom interfacial layer is less than 0.4 nm thin. The scaling potential combined with the high mobility of the Ge substrate makes the Ge/high-κ stacks promising for high-performance complementary metal-oxide semiconductor (CMOS) applications.

ACKNOWLEDGMENTS

Jan Vansteenbergen is acknowledged for substantial assistance with Ge substrate cleaning. Jan Willem Maes, Otto Laitinen, and Hilde De Witte (ASM Belgium) are kindly acknowledged for their contribution in the preparation of the HfO_2 samples. The authors are grateful to Umicore for providing the Ge substrates. Cees van der Marel and Paul Pijpers from Philips Electronics Nederland B.V., Eindhoven are kindly acknowledged for XPS analysis of the Ge/HfO_2 samples. One of the authors (R.L.P) acknowledges a post-

Downloaded 16 Sep 2008 to 129.100.41.190. Redistribution subject to AIP license or copyright; see http://jap.aip.org/jap/copyright.jsp

doctoral fellowship by IMEC/K.U. Leuven and support from the Academy of Finland (Grant Nos. 105364 and 202633).

[1]C. O. Chui, H. Kim, D. Chi, B. B. Triplett, P. C. McIntyre, and K. C. Saraswat, Tech. Dig. - Int. Electron Devices Meet. **2002**, 437.
[2]S. M. George, A. W. Ott, and J. W. Klaus, J. Phys. Chem. **100**, 13121 (1996).
[3]M. Ritala and M. Leskelä, in *Handbook of Thin Film Materials*, edited by H. S. Nalwa (Academic, New York, 2002), Vol. 1, p. 103.
[4]M. L. Green *et al.*, J. Appl. Phys. **92**, 7168 (2002).
[5]A. Satta *et al.*, J. Appl. Phys. **92**, 7641 (2002).
[6]R. L. Puurunen, Chem. Vap. Deposition **9**, 249 (2003).
[7]R. L. Puurunen, Chem. Vap. Deposition **10**, 159 (2004).
[8]R. L. Puurunen, J. Appl. Phys. **95**, 4777 (2004).
[9]H. Lüth, *Surfaces and Interfaces of Solids* (Springer, Berlin, 1993), p. 94.
[10]M. A. Alam and M. L. Green, J. Appl. Phys. **94**, 3403 (2003).
[11]M. Caymax *et al.*, *ALD2002 Conference*, 19–21 August 2002, Seoul, Korea (unpublished).
[12]S. Haukka, M. Tuominen, E. Vainonen-Ahlgren, E. Tois, and W.-M. Li, *203th meeting of the Electrochemical Society*, 24 April–2 May 2003 Paris, France (unpublished).
[13]A. Delabie *et al.*, Mater. Res. Soc. Symp. Proc. **745**, 179 (2003).
[14]D. Blin *et al.*, *203th Meeting of the Electrochemical Society*, 24 April–2 May 2003, Paris, France (unpublished).
[15]E. P. Gusev, C. Cabral, Jr., M. Copel, C. D'Emic, and M. Gribelyuk, Microelectron. Eng. **69**, 145 (2003).
[16]W. Vandervorst *et al.*, Mater. Res. Soc. Symp. Proc. **745**, 23 (2003).
[17]H. Bender *et al.*, Proc.-Electrochem. Soc. **3**, 223 (2003).
[18]T. Conard, W. Vandervorst, J. Petry, C. Zhao, W. Besling, H. Nohira, and O. Richard, Appl. Surf. Sci. **400**, 203 (2003).
[19]ALCVD™ and Polygon™ 8200 are trademarks of ASM International nv.
[20]P. S. Cumpson, Surf. Interface Anal. **29**, 403 (2000).
[21]S. Tanuma, C. J. Powell, and D. R. Penn, Surf. Interface Anal. **21**, 165 (1994).
[22]F. van der Veen, Surf. Sci. Rep. **5**, 199 (1985).
[23]T. Gustafsson, H. C. Lu, B. W. Busch, W. H. Schulte, and E. Garfunkel, Nucl. Instrum. Methods Phys. Res. B **183**, 146 (2001).
[24]R. M. Tromp, M. Copel, M. C. Reuter, M. Horn von Hoegen, J. Speidell, and R. Koudijs, Rev. Sci. Instrum. **62**, 2679 (1991).
[25]W. H. Schulte, B. W. Busch, E. Garfunkel, T. Gustafsson, G. Schiwietz, and P. L. Grande, Nucl. Instrum. Methods Phys. Res. B **1883**, 16 (2001).
[26]R. C. Weast and M. J. Astle, *CRC Handbook of Chemistry and Physics* (CRC, Florida, 1994), p. B-73–166.
[27]G. C. van Leerdam, K.-M. H. Lenssen, and H. H. Brongersma, Nucl. Instrum. Methods Phys. Res. B **45**, 390 (1990).
[28]S. Ferrari, G. Scarel, C. Wiemer, and M. Fanciulli, J. Appl. Phys. **92**, 7675 (2002).
[29]C. Zhao, G. Roebben, M. Heyns, and O. van der Biest, Key Eng. Mater. **206**, 1285 (2002).
[30]S. M. Cohen, Y. L. Yang, E. Rouchouze, T. Jin, and M. P. D'Evelyn, J. Vac. Sci. Technol. A **10**, 2166 (1992).
[31]J. Y. Lee, J. Y. Maeng, A. Kim, Y. E. Cho, and S. Kim, J. Chem. Phys. **118**, 1929 (2003).
[32]L. Pagagno, X. Y. Shen, J. Anderson, G. Schirripa Spagnolo, and G. J. Lapeyre, Phys. Rev. B **34**, 7188 (1986).
[33]Y. J. Chabal, G. S. Higashi, K. Raghavachari, and V. A. Burrows, J. Vac. Sci. Technol. A **7**, 2104 (1989).
[34]D. W. Greve, Mater. Sci. Eng., B **18**, 22 (1993).
[35]M. de Ridder *et al.*, J. Phys. Chem. B **106**, 13146 (2002).
[36]R. L. Puurunen and W. Vandervorst, J. Appl. Phys. **96**, 7686 (2004).
[37]H. Bender *et al.*, in *Extended Abstracts of International Workshop on Gate Insulator*, edited by M. Hirose, S. Sakai, and H. Iwai (Business Center for Academic Societies Japan, Tokyo, 2001), p. 86.
[38]J. W. Elam, C. A. Wilson, M. Schuisky, Z. A. Sechrist, and S. M. George, J. Vac. Sci. Technol. B **21**, 1099 (2003).
[39]H. Kim, C. O. Chui, K. C. Saraswat, and P. C. McIntyre, Appl. Phys. Lett. **83**, 2647 (2003).
[40]G. E. Rodgers, *Introduction to Coordination, Solid State, and Descriptive Inorganic Chemistry* (McGraw–Hill, Singapore, 1994), p. 164.
[41]For example, the RBS Hf coverage and LEIS HfO_2 surface fraction in the first cycle can be reproduced assuming a cylindrical shape of the HfO_2 islands with height of 1 nm and radius 0.3 nm, with a distribution of one island per nm^2. The cylindrical configuration would allow a much higher maximum Cl coverage, of about 23 Cl/nm^2.
[42]S. Haukka, E.-L. Lakomaa, and A. Root, J. Phys. Chem. **97**, 5085 (1993).
[43]S. Haukka, E.-L. Lakomaa, O. Jylhä, J. Vilhunen, and S. Hornytzkyj, Langmuir **9**, 3497 (1993).
[44]P. J. Kooyman, P. van der Waal, P. A. J. Verdaasdonk, K. C. Jansen, and H. van Bekkum, Catal. Lett. **13**, 229 (1992).
[45]A. Kytökivi, E.-L. Lakomaa, and A. Root, Langmuir **12**, 4395 (1996).
[46]M. Ritala and M. Leskelä, Thin Solid Films **225**, 288 (1993).
[47]M. Ritala, M. Leskelä, L.-S. Johansson, and L. Niinistö, Thin Solid Films **228**, 32 (1993).
[48]M. Ritala and M. Leskelä, Appl. Surf. Sci. **75**, 333 (1994).
[49]M. Ritala, M. Leskelä, L. Niinistö, T. Prohaska, G. Friedbacher, and M. Grassenbauer, Thin Solid Films **250**, 72 (1994).
[50]M. Caymax *et al.*, Mater. Res. Soc. Symp. Proc. **765**, D2.6.1 (2003).
[51]S. Van Elshocht, Mater. Res. Soc. Symp. Proc. **809**, 287 (2004).
[52]W. F. A. Besling *et al.*, J. Non-Cryst. Solids **303**, 123 (2002).

Downloaded 16 Sep 2008 to 129.100.41.190. Redistribution subject to AIP license or copyright; see http://jap.aip.org/jap/copyright.jsp